Talanta 118 (2014) 262–269

Contents lists available at ScienceDirect

Talanta

journal homepage: www.elsevier.com/locate/talanta

Functionalized gold nanoparticles for the detection of arsenic in water

R. Domínguez-González, L. González Varela, P. Bermejo-Barrera *

Department of Analytical Chemistry, Nutrition and Bromatology, Faculty of Chemistry, 15782 Santiago de Compostela, Spain

ARTICLE INFO

Article history:
Received 20 May 2013
Received in revised form
3 October 2013
Accepted 15 October 2013
Available online 23 October 2013

Keywords:
Gold nanoparticles
Arsenic
Water
VIS Spectroscopy

ABSTRACT

Gold nanoparticles are attractive as sensing materials because of their size and shape are related with their optical properties. The color change produced by the aggregation of functionalized AuNPs allows the detection of arsenic at low levels. A simple, cheap and fast analytical procedure to perform arsenic determination using functionalized gold nanoparticles (AuNPs) and VIS spectrometry as a detection technique is studied. Three different synthesis procedures to obtain the AuNPs and two different functionalization modes were studied. AuNPs functionalized with GSH-DTT-CYs-PDCA were selected as the most adequate. The correlation between the decrease in the absorbance signal and the arsenic concentration was good in the 2–20 $\mu g\, l^{-1}$interval. Repeatability, expressed as average of RSD (%), obtained for the different arsenic concentrations studied was 0.6%. The average value of the analytical recovery was 99.7%. The detection and quantifications limits were 2.5 and 8.4 $\mu g\, l^{-1}$ respectively. These limits are sufficient to detect World Health Organization's guideline value of 10 $\mu g\, l^{-1}$.

1. Introduction

The presence of arsenic in the environment is associated with geological and anthropogenic sources, being drinking water the main route of arsenic exposure. Although arsenic levels in natural water are usually low, in some areas, due to geological sources, groundwater presents levels higher than that recommend by the World Health Organization (WHO) of 10 $\mu g\, L^{-1}$ [1]. Nowadays, aproximately 140 million people are in risk of being exposed to drinking water with high arsenic levels. Some areas of Banglasdesh [2], Taiwan [3], Argentina [4], Chile [5] and the US [6] present this problem. Arsenic in mineral and sedimentary deposits can be released as inorganic arsenic into groundwater under certain conditions. In groundwater, As is mostly present as As (V) [7] but can be reduced to As (III) [7] under anaerobic conditions. Inorganic arsenic compounds are classified by the International Agency for Research on Cancer (IARC) in Group 1 (carcinogenic to humans), on the basis of sufficient evidence for carcinogenicity in humans and limited evidence for carcinogenicity in animals [8]. A report of the International Programme on Chemical Safety (IPCS) [9] concluded that long-term exposure to arsenic in drinking water may be related to increased risks of cancer in the skin, lungs, bladder and kidneys, as well as other skin problems, such as hyperkeratosis and pigmentation changes. Due to these problems, the control of the arsenic levels in drinking waters is essential. Different analytical techniques such as Electrothermal Atomization Atomic Absorption Spectroscopy (ETAAS) [10,11], Hydride Generation coupled to Atomic Absorption Spectroscopy (HG-AAS) [12], or coupled to Atomic Fluorescence Spectroscopy (HG-AFS) [13], Mass Spectrometry with Inductively Coupled Plasma, ICP-MS [14], certain electrochemical methods [15,16], and Spectrofluorimetry [17] have been used to perform arsenic determination at low levels. Nevertheless, a pre-concentration step is sometimes necessary, and in many cases these techniques are not available, mainly in underdeveloped countries.

For this reason, new methods that allow real-time detection of arsenic at $\mu g\ l^{-1}$ levels have been developed in recent years [18–22]. The use of nanomaterials has increased in many fields due to their optical, electronic, magnetic and catalytic properties. These materials include gold nanoparticles (AuNPs) among others. These particles present interesting optical properties due to their strong surface plasmon resonance (SPR) absorptions in the visible region, and their ease of preparation and stability. The SPR absorption wavelength of AuNPs depends among other factors on the size, shape and refractive index; therefore, any changes in these properties may lead to colorimetric changes. On the other hand, due to the properties of the AuNPs surface is possible the linking of different functional groups. This can be possible through strong bonding between Au–S or Au–N, or through physical adsorption processes [23–25].

Due to the high molar absorptivities and the relation between the optical properties and AuNPs sizes, most AuNPs sensors are used in colorimetric modes. One of the applications of these sensors, based on the color changes produced by the AuNPs aggregation, is to detect metal ions [26–30]. In a recent review the use of the AuNPs sensors for the detection of mercury, lead and

* Corresponding author. Tel.: +34881814266, fax: +34547141.
E-mail address: pilar.bermejo@usc.es (P. Bermejo-Barrera).

0039-9140/$ - see front matter © 2013 Elsevier B.V. All rights reserved.
http://dx.doi.org/10.1016/j.talanta.2013.10.029

copper was discussed [31]. The principal factors that affect sensitivity and selectivity of these sensors are size and concentrations of AuNPs, the nature of the molecule for the recognition of the element, pH, ionic strength, buffer solution and the temperature. The aim of this paper is to develop a simple and inexpensive method for the arsenic determination in water samples at low levels using AuNPs and VIS Spectroscopy as a detection technique.

2. Materials and methods

2.1. Apparatus

UV–vis spectrophotometer U-2010 (Hitachi, USA) was used to record UV–vis absorption spectra at room temperature from 900 to 400 nm. The Transmission Electron Microscopy (TEM) images of the nanoparticles were acquired on a JEM 2010 transmission electron microscope with the voltage of 120 kV (JEOL). A Boxcult incubator situated on a Rotabit orbital-rocking platform shaker (J.P. Selecta, Spain) was used to perform the nanoparticles modification. All pH values were measured with a Basic 20 pH meter (Crison Instruments, Spain).

2.2. Reagents

Gold (III) chloride trihydrate (99.9%), sodium citrate dihydrate (99.8%), Glutathione (GSH), DL-dithiothreitol (DTT, 99.5%), L-cysteine (98.5%), 2,6-pyridinedicarboxylic acid (PDCA, 99.5%) were purchased from Sigma-Aldrich, sodium borohydride (98%) were from Alfa Aesar. Arsenic (As_2O_3, Sigma-Aldrich) was used as standard. Nitric acid (65%), hydrochloric acid (37%) used for cleaning procedure were purchase from Panreac.

Ultrapure water of 18 MΩcm obtained from a Milli-Q water purification system (Millipore Corp., Bedford, MA, USA) was used throughout the work.

2.3. Cleaning procedure

All glassware and storage bottles were kept in 10% nitric acid for at least 48 h, rinsed three times with ultrapure water, and preserved dry until used. All the material used with nanoparticles were cleaned with aqua regia and rinsed with ultrapure water.

2.4. Procedures

2.4.1. Synthesis of gold nanoparticles (AuNPs)

To perform the AuNPs synthesis, 4.6 ml of $HAuCl_4.3H_2O$ solution (0.1 M) was added to 85 ml of ultrapure water; afterwards, 5 ml of freshly prepared sodium citrate (10^{-2}M) solution was added while stirring. To end, 5 ml of freshly prepared sodium borohydride (0.1 M) solution in ice bath were added drop by drop with constant stirring at low temperature. The solution was keep refrigerated overnight under static conditions.

2.4.2. Functionalization of gold nanoparticles

The modified AuNPs were obtained by addition of 500 μl of GSH (10 mM), 500 μl of DTT (10 mM) and 500 μl of Cys (12 μM) solutions to 100 ml of AuNPs solution. This solution was introduced for 2 h in a Boxcult incubator at room temperature with orbital-rocking shaking (150 rpm) in dark conditions. The solution was refrigerated overnight. Afterwards, 500 μl of PDCA (10 mM) solution were added while stirring and kept in dark and static conditions at least 2 h until use.

The stability of AuNPs functionalized was study. During 1 month the Absorbance was measured at 525 nm and the analytical signal remains constant (RSD=0.5%) in the studied period.

2.4.3. As determination with UV–vis detection

To perform the analysis of As with AuNPs by VIS spectroscopy 1 ml of standard/sample (pH=9.3) was added to 2 ml of modified AuNPs. Calibration curves were made with As standards between 2 and 20 μg/l at the wavelength of the absorbance maximum. Quartz cells (1 cm path length) were used to spectrometric measurements because the plastic cells get stained with use.

3. Results and discussion

3.1. Study of the gold nanoparticles synthesis

The most common and simplest procedure to obtain AuNPs is the aqueous reduction of $HAuCl_4$ by sodium citrate at solutions boiling point [32,33]. This method produces monodisperse spherical AuNPs in the range of 10–20 nm diameters. This size is related with the citrate/gold molar ratio. The reducing agent used to obtain the nanoparticles acts not only as reducing agent, but also as capping agents that stabilize the nanoparticles formed. Borohydride has been proposed among others possible reducing agents in aqueous phase [34]. Moreover, other reducing agents have been proposed in recent years, as we can see in the review of the Lin [29]. In this work the AuNPs were obtained after reduction of Au (III) ($HAuCl_4.3H_2O$) with sodium citrate and sodium borohydride following the proposed method by Darbha [35]. On the other hand the size of the nanoparticle synthesized depends on the concentrations of the reagents used in the synthesis procedure; therefore, we studied the effect of the different reagents amounts on the particle size. Using the same procedure described in Section 2.4.1, three different synthesis experiments using different amounts of reagents were performed; the amounts of reagents used are shown in Table 1.

3.1.1. Characterization of the AuNPs obtained in the different synthesis procedures using transmission electron microscopy (TEM)

To perform the AuNPs characterization by using Transmission Electron Microscopy (TEM), a JEM 2010 (JEOL) instrument operating at a voltage of 120 kV was used. Samples were prepared by depositing a drop of a solution on a carbon-coated Cu grid (3 mm diameter) and dried at room temperature. The AuNPs formed following the procedures studied before (S1, S2 and S3) were investigated by TEM (Fig. 1). The diameters of the AuNPs were measured with the Image Tool program. The mean diameters, the diameter size frequency in the samples and the corresponding histogram were obtained with Statgraphic Plus. TEM images and histograms are shown in Fig. 1.

The smallest particles (mainly spherically shaped) with a mean size of 4.7 ± 0.77 nm and with short size dispersion were obtained after performing the S1 synthesis procedure. Regarding S2 synthesis, TEM showed nanoparticles with larger mean particle size and size dispersion (9.4 ± 2.1 nm). S3 synthesis produced similar results that those obtained with S2 synthesis (nanoparticles size dispersion of 10 ± 2.5 nm). For S2 nd S3 synthesis procedures we can also observed that the shape of the particles was not always spherical.

Table 1
Reagent concentrations used in the synthesis of the gold nanoparticles.

Reagent	Synthesis 1, S1 (M)	Synthesis 2, S2 (M)	Synthesis 3, S3 (M)
Sodium citrate	2.49×10^{-4}	5.02×10^{-4}	2.04×10^{-3}
Sodium borohydride	2.49×10^{-3}	5.02×10^{-3}	2.49×10^{-3}
Gold (III) chloride	2.51×10^{-4}	5.03×10^{-4}	2.74×10^{-4}

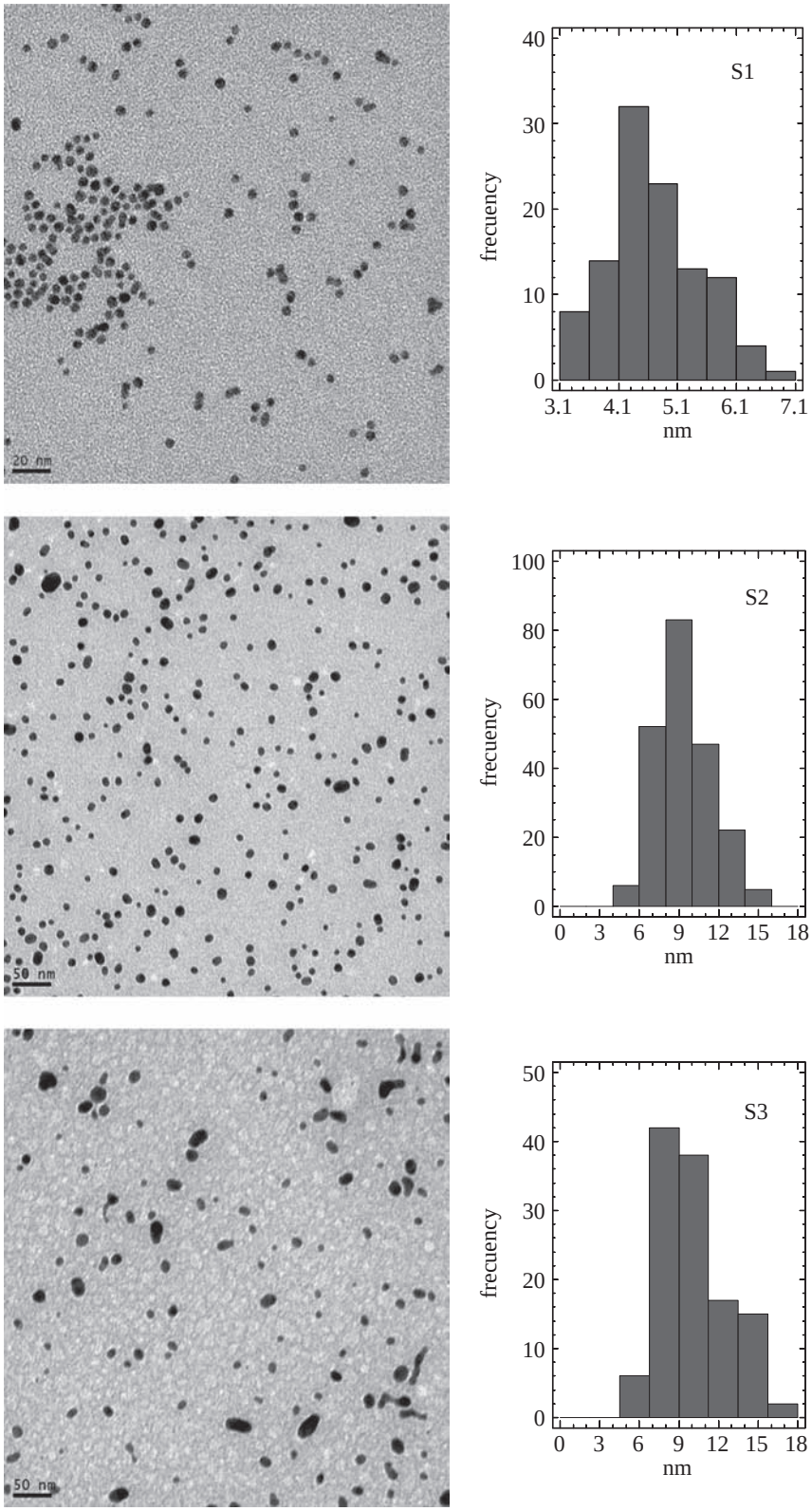

Fig. 1. TEM images and the corresponding histograms of AuNPs obtained by S1, S2 and S3 synthesis procedures.

3.1.2. Characterization of the AuNPs by VIS spectrometry

Visible absorption spectrums were obtained from 400 to 900 nm for the particles from the three synthesis procedures. In Fig. 2 we can see the absorption spectra, the maximum wavelength of the plasmon band, and the color. Plasmon bands maximum at 505, 515 and 525 nm, and with absorbance values of 0.753, 1.780 and 0.859 were obtained for S1, S2 and S3 respectively. Small plasmon band shifts from 505 (S1) to 525 (S3) were observed. The results obtained show difference absorbance values for three synthesis procedures. Higher absorbance values for S2 were observed, this effect is probably due to the higher Au concentration used.

The results obtained in these studies are no conclusive for the selection of the best synthesis procedure; therefore the three procedures will be used in the study of the functionalization of the AuNPs.

3.2. Functionalization of the AuNPs

In order to achieve high selectivity for arsenic determination, the AuNPs must be subjected to modification with recognition elements that interact selectively with the arsenic. Moreover, due since many recognition elements are bound to each nanoparticle, multivalent effects are possible which can produce an increase in sensitivity. But in some cases, if the density of the recognition elements on the nanoparticle is too high, some problems related with the steric effects can be produced. Another important aspect is the orientation of the recognition elements on the nanoparticle surface. In some cases, the space between the thiol group or the nitrogen group and the recognition element requires to have a certain orientation for obtaining a nanoparticle with high functionality. Different types of interactions can occur between the nanoparticles and the recognition element (physical interactions: electrostatic and hydrophobic; interactions with covalent coupling: for example Au–S covalent bonds or specific recognition interactions, such as antibody–antigen). The process of physical interactions is fast and simple, but ligands can be released into the bulk solution when changes in the experimental conditions occur. Therefore, the strong bonds such as those between Au and S are preferred. In recent years the modification of the AuNPs has been performed with different compounds, such as carbohydrates [36], mercaptopropionic acid (MPA) with homocystine (HCys) and the chelating agent PDCA (2,6-pyridinedicarboxilic acid) [35], glutathione (GSH) [37,38] and GSH with dithiothreitol (DTT) cysteine (Cys) [39].

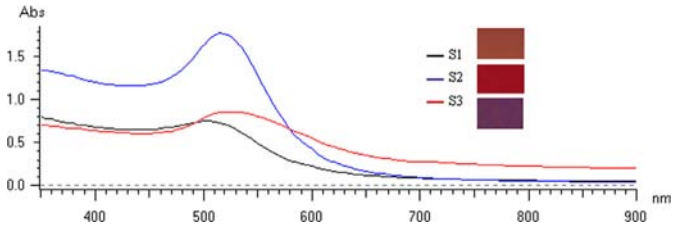

Fig. 2. VIS absorption spectra of AuNPs synthesized using the three synthesis procedures, S1, S2 and S3, and the corresponding color of the AuNPs solutions.

In the present work the effect of functionalizing the AuNPs using GSH, DTT and Cys as modifier (Modification 1, M1) was studied. On the other hand, to avoid the interference effect produced by mercury [39], AuNPs functionalized with GSH-DTT-Cys-PDCA (Modification 2, M2) was prepared. In the GSH-DTT-Cys modification (M1), 500 μl of GSH (10 mM), 500 μl of DTT (10 mM) and 500 μl of Cys (12 μM) were added to 100 ml of each AuNPs' solutions. These solutions were introduced for 2 h in a Boxcult incubator at room temperature and with orbital-rocking shaking (150 rpm) in dark conditions and kept refrigeration overnight. The procedure for GSH-DTT-Cys-PDCA modification (M2) begins with the same procedure (M1) and after 2 h in dark and static conditions followed with the addition of 500 μl of PDCA (10 mM), stirring and keep in dark and static conditions at least for 2 h until use. We performed the two modification procedures for the three possible synthesis methods described above. The particle and shape of the nanoparticle was studied by TEM and by VIS Spectroscopy.

3.2.1. Characterization of the functionalized AuNPs using the transmission electron microscopy (TEM)

The AuNPs synthesized by procedures S1, S2 and S3 and modified using GSH-DTT-CYS (M1) and GSH-DTT-CYS-PDCA (M2), were studied by TEM. The TEM images and their corresponding histograms of AuNPs size distributions are shown in Figs. 3–5. For the AuNPs synthesized by procedure S1, the change in the AuNPs size was from 4.7 ± 0.77 nm without modification, to 4.1 ± 0.75 and 4.3 ± 0.80 nm after M1 and M2 modifications respectively. For the synthesized AuNPs by procedure S2 the change in the AuNPs size was from 9.4 ± 2.1 nm without modifications to 7.7 ± 1.7 and 7.7 ± 1.4 nm after M1 and M2 modifications respectively. For the AuNPs synthesized by procedure S3 the changes in the AuNPs size were from 10.1 ± 2.5 nm without modifications to 9.1 ± 1.6 and 9.2 ± 1.9 nm after M1 and M2 modifications respectively.

A one way variance analysis (ANOVA) shows statistically significant differences (95% confidence level) between AuNPs sizes before and after modification; a decrease in the particle size was observed in all cases. A Multiple Range Test (employing the least significant difference Fisher (LSD)) shows that there are significant differences (95% confidence level) between the means of the AuNPs's diameters obtained before and after applying the different modification procedures in all cases, but there are no significant differences in size between the modification procedures used in all the synthesis studied.

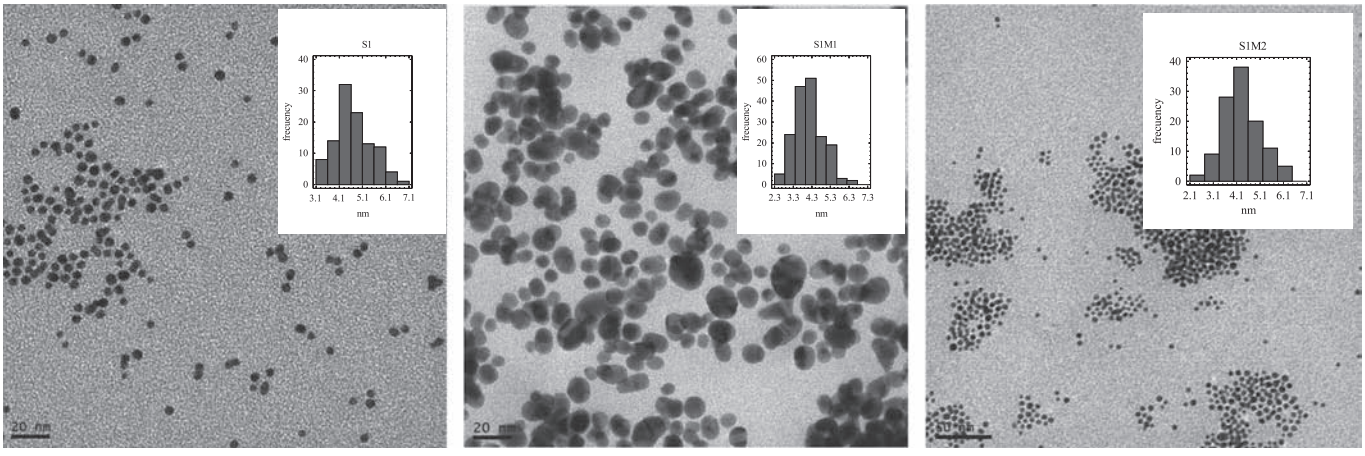

Fig. 3. TEM images of AuNPs obtained by the synthesis procedure S1 before and after modification procedures M1 and M2, and their corresponding histograms of distribution of AuNPs.

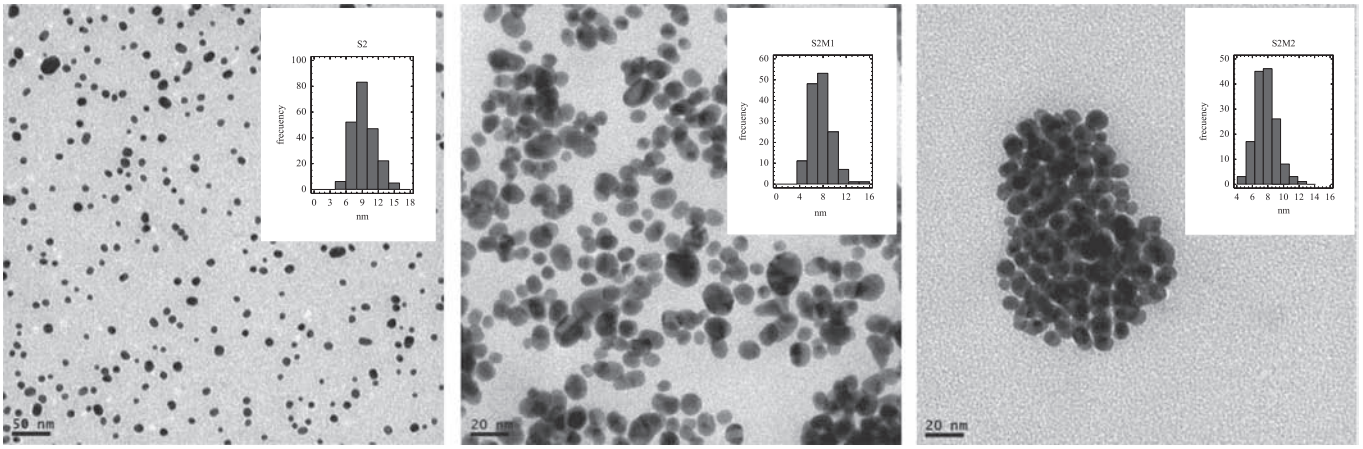

Fig. 4. TEM images of AuNPs obtained by the synthesis procedure S2 before and after modification procedures M1 and M2, and their corresponding histograms of distribution of AuNPs.

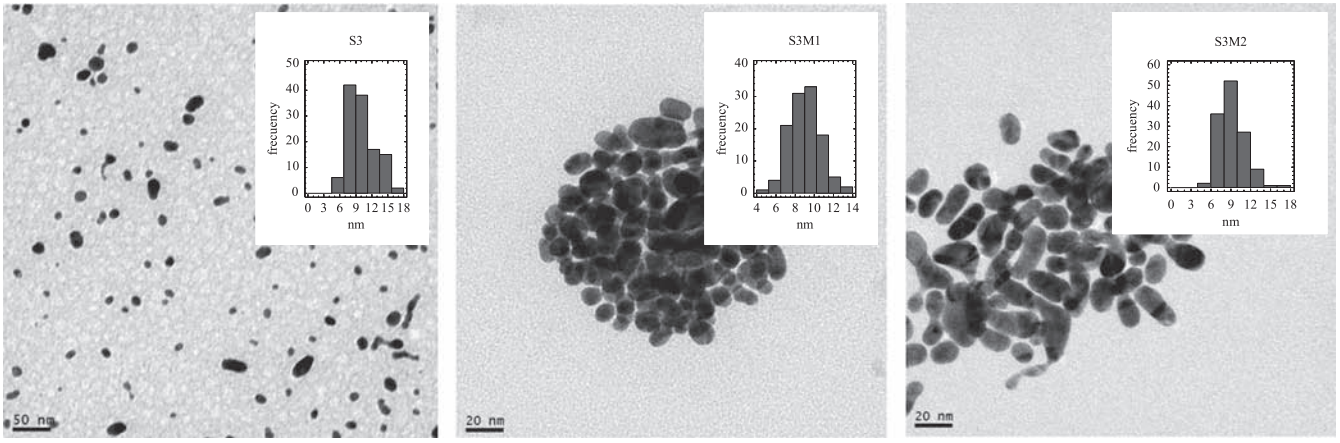

Fig. 5. TEM images of AuNPs obtained by the synthesis procedure S3 before and after modification procedures M1 and M2, and their corresponding histograms of distribution of AuNPs.

3.2.2. *VIS absorption spectra of modified AuNPs*

The synthesized AuNPs following S1, S2 and S3 procedures before and after modification by M1 and M2 procedures were analyzed by VIS spectrometry; results are shown in Fig. 6 and in Table 2. First we can observe the plasmon band shifts slightly from 505 to 510 nm and from 515 to 525 nm for the S1 and S2 procedure synthesis, respectively. The type of modifications, however did not change the maximum wavelength of the plasmon band. For S3 procedure there is no change in the wavelength in the presence of the modification agents. On the other hand, a decrease in the absorbance has been observed for the different synthesis procedures. The most important decrease (12%) was observed with the S1 procedure. A decrease of 10 and 5% was observed with the S3 and S2 procedures respectively.

3.3. *Arsenic determination using functionalized AuNPs by VIS spectroscopy*

Arsenic determination using functionalized AuNPs by VIS spectroscopy is based on the aggregation of modified nanoparticles in the presence of arsenic (III). This aggregation produced a color change and a variation in the absorbance signal in the VIS region. When modification of the AuNPs with DDT was used, this agent acts not only as a modifier but also transform As(V) to As(III) [39], thus making possible the determination of total inorganic arsenic in a sample.

3.3.1. *Study of arsenic determination by VIS spectroscopy using the AuNPs modified with GSH-DTT-Cys*

Due to the differences in the particle size of the AuNPs obtained with the three synthesis procedures, we studied the calibration curves using nanoparticles synthesized by the three proposed procedures. To perform the calibration curves for As determination, 1 ml of arsenic standard solution was added to 2 ml of modified AuNPs. Calibration curves were plotted for the maximum absorbance signal (A) obtained for each synthesis procedure versus standard concentration between 20 and 200 $\mu g\, l^{-1}$. The linearity of the response (A versus concentration) was verified in the whole range of concentrations studied. The correlation coefficients R^2 obtained were always >0.998.

Moreover, addition curves were performed with tap water samples and the slopes obtained were similar to the aqueous calibration slopes when using AuNPs obtained after all three synthesis procedures.

The limit of detection (LOD) and the limit of quantification (LOQ), defined as 3SD/m and 10SD/m, respectively, where SD is the standard deviation of the blank ($n=11$) and m is the slope of calibration graph, are listed in Table 3. The lowest LOD and LOQ were observed for the nanoparticles obtained with the S2 synthesis procedure.

Repeatability was obtained by independent trials of the same method ($n=10$), in the same laboratory by the same operator, under these conditions the RSD average (%) obtained for the different levels of arsenic concentration studied were 0.8,

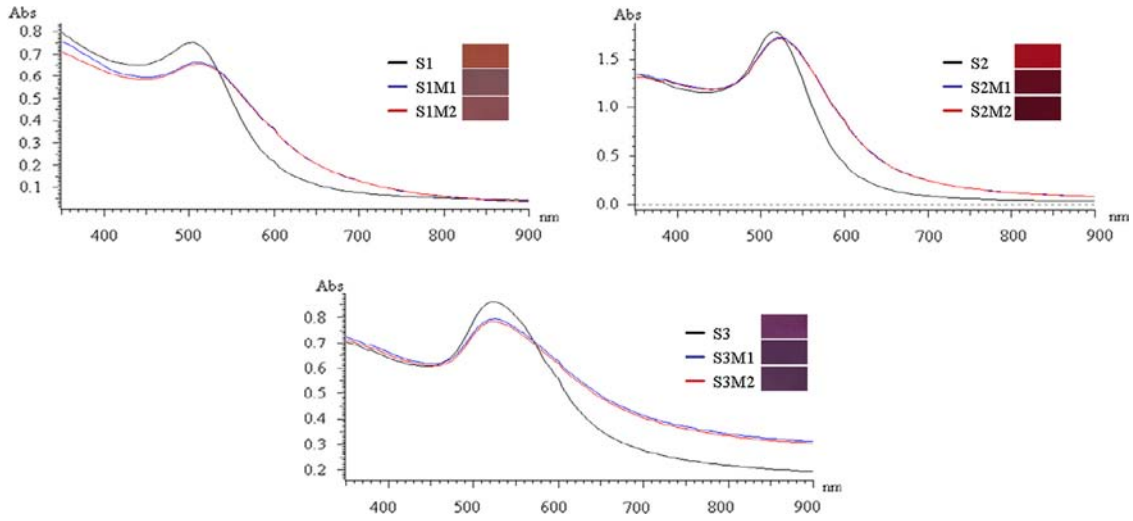

Fig. 6. VIS absorption spectra of AuNPs synthesized by S1, S2 and S3 before and after modification procedures M1 and M2, and solutions color.

Table 2
Maximum wavelength (λ_{max}(nm)) and Absorbance at this λ_{max} (A) obtained for AuNPs synthesized by S1, S2 and S3 procedures before and after modification M1 and M2 procedures.

Parameter	Synthesis 1			Synthesis 2			Synthesis 3		
	S1	S1M1	S1M2	S2	S2M1	S2M2	S3	S3M1	S3M2
λ_{max}(nm)	505	510	510	515	525	525	525	525	525
A	0.753	0.664	0.657	1.780	1.721	1.710	0.859	0.794	0.784

Table 3
Figures of merit obtained for the different procedures of synthesis studied (S1, S2 and S3) with the GSH-DTT-Cys modification (M1). LOD-limit of detection, LOQ-limit of quantification, R-analytical recovery.

Procedure	LOD (μg l^{-1})	LOQ (μg l^{-1})	R (%)
S1M1	100	400	128.2
S2M1	20	60	93.9
S3M1	100	500	77.4

0.5 and 2% for S1M1, S2M1 and S3M1, respectively. The precision was very good in all procedures studied, but the best results were obtained for the S2 synthesis procedure with a RSD value of 0.5%.

The analytical recovery was studied for water samples at different As levels to evaluate the accuracy of methods. The average value of analytical recovery (*R*%) for the different procedures studied is also shown in Table 3. The best results were obtained for the S2M1 synthesis procedure with a recovery value of 93.9%.

3.3.2. *Study of arsenic determination by VIS spectroscopy using the AuNPs modified with GSH-DTT-Cys-PDCA*

To perform the study of As determination using the AuNPs modified with GSH-DTT-Cys-PDCA, and in order to know which is the most adequate amount of PDCA, a study on the effect of the amount of PDCA on the calibration curves and on the sensitivity and precision was performed. To perform this study, amounts of PDCA of 5×10^{-5}, 5×10^{-4} and 3×10^{-3} M was used. In all cases, a linear relationship between the arsenic and the absorbance was obtained with good correlation coefficients. At the highest level of PDCA, the plasmonic band drifts from 515 to 560 nm in S1M2, and from 525 to 560 nm in S2M2 and S3M2. The LOD, LOQ and RSD obtained in all cases are listed in Table 4. The best detection limits obtained for As determination with AuNPs were 21, 12 and

Table 4
Figures of merit obtained for the different procedures of synthesis studied (S1, S2 and S3) with GSH-DTT-Cys-PDCA modification (M2) at different concentration levels; A – 5×10^{-5}M B – 5×10^{-4}M, C – 3×10^{-3}. LOD-limit of detection, LOQ-limit of quantification.

Procedure	PDCA,M	LOD (μg l^{-1})	LOQ (μg l^{-1})	RSD (%)
S1M2	A	21	70	0.2
	B	21	71	0.2
	C	21	71	0.6
S2M2	A	12	40	0.2
	B	28	94	0.2
	C	339	1131	10
S3M2	A	11	35	0.2
	B	64	212	0.9
	C	7	24	1.9

11 μg l^{-1} for S1M2, S2M2 and S3M2, respectively. These limits were better than those obtained previously with the modification M1 (Table 3). Although a LOD of 7 μg l^{-1} was obtained for S3M2 using the highest amount of PDCA, in this case the precision was worse, thus the lower amount of PDCA was the most adequate. Under these conditions, precision was very good, the RSD average (%) obtained for the different arsenic levels ($n=10$) was 0.3%. The analytical recovery studied for water samples at the same As levels as before is good. The average value of analytical recovery (*R*%) for S2M2 was 95%.

After this study we selected the synthesis 2 procedure and the modification 2 (S2M2) of the AuNPs with GSH-DTT-Cys-PDCA as the most adequate.

3.3.3. *Effect of pH*

In recent years different studies have demonstrated that the pH of the precursor solutions is an important factor that can

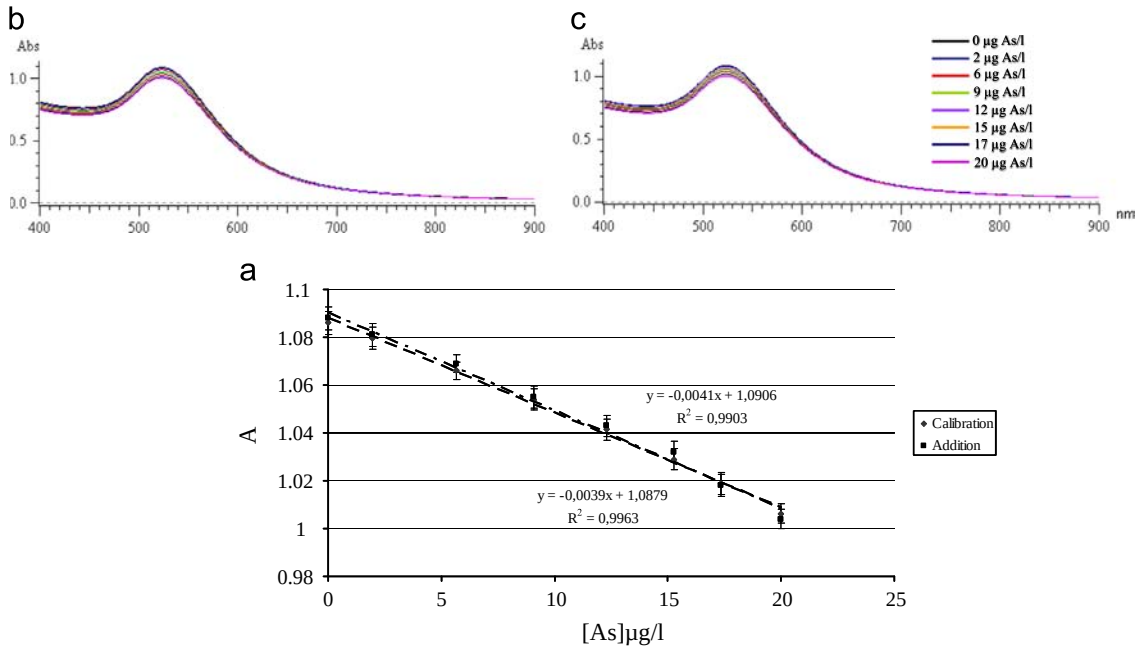

Fig. 7. Calibration and addition curves to As determination obtained with AuNPs modified with GSH-DTT-Cys-PDCA after adjust pH to 9 of Milli-Q water and sample used in calibration and addition solutions respectively.

determine the particle size and size distribution of citrate-AuNPs [40,41]. On the other hand, the pH change produced with the addition of standards or samples can also affect the nanoparticles aggregation. The AuNPs modified with GSH-DTT-Cys-PDCA present a pH of 9.3, but the water used to prepare the standards for calibration and the pH of real water samples is lower than this pH. Thus, to know the possible effect of the standards and samples pHs we performed a study varying the standards and water samples pH between 4.5 and 10, using sodium hydroxide 0.5 M to obtain the different pH values. The best results (a higher absorbance signal) were obtained when standards and water samples present the same pH as the AuNPs, therefore we selected 9.3 as the most adequate pH.

3.4. Analytical characteristics of the method for arsenic determination in water samples using the AuNPs modified with GSH-DTT-Cys-PDCA

To obtain the calibration graph the arsenic concentration was varied between 2 and 20 $\mu g\, l^{-1}$. Fig. 7(a) shows the calibration graph and the addition graph obtained with a real water sample. The regression coefficient were higher than 0.99 in both cases, and there is no significant difference between the slopes of calibration and addition graphs. Absorbance spectrums obtained in the same conditions are shown in Fig. 7(b) and (c).

Repeatability expressed as average of RSD (%) obtained for the different arsenic levels of concentration studied was 0.6%.

The analytical recovery was studied for water samples at the different arsenic levels to evaluate the accuracy of the method. The average value of analytical recovery (*R%*) at the different arsenic levels studied was 99.7%.

The detection and quantifications limits were 2.5 and 8.4 $\mu g\, l^{-1}$, respectively. These limits are sufficient to detect World Health Organization's guideline value of 10 $\mu g\, l^{-1}$.

On the other hand, an interference study on the principal trace elements that are present in drinking water was performed. To perform this study a water sample spiked with different amounts of the interfering element was prepared, and the absorbance was measured using the proposed procedure. We consider that an element produces an interference when a change in the absorbance signal higher than 1% is produced. In Table 5, we can see the levels of the different elements that did not produce interferences. There are no interferences at the maximum allowed levels, legislation of the government of Spain [42], for all studied elements except for the selenium. Although it is necessary to perform more studies to avoid this problem, in general the selenium levels in drinking water are lower than the selenium level that produces an interference.

Table 5
Study of interferences for different elements on the arsenic signal.

Element	Allowed level or (guideline level), µg/l	Maximum element concentration that did not produce interference, µg/l
Ca	(11×10^3 to 160×10^3)	4200
Cd	5	5
Co	–	4200
Cu	(100)	8000[a]
Fe	(50)	48
Mg	(30)	4000
Mn	(20)	38
Na	–	900
Ni	20	5000
Pb	10	9
Se	10	2
Zn	(100)	48

[a] The highest level studied was 8 µg/ml.

4. Conclusions

In this paper a simple method to perform the arsenic determination in water at $\mu g\, l^{-1}$ levels using VIS spectroscopy has been developed. The method is based on the absorbance decrease of the AuNPs functionalized with GSH-DDT-CYs-PDCA in the presence of arsenic. The method presents a Detection Limit of 2.5 $\mu g\, l^{-1}$ that is sufficient to detect the World Health Organization's guideline

value of 10 μg l^{-1}. The precision is good with a RSD average of 0.6% and the method presents a recovery of 99.7%.

Acknowledgments

The authors wish to acknowledge the Xunta de Galicia (Project number 10PXIB209032PR) for financial support.

References

[1] ⟨http://www.who.int/water_sanitation_health/dwq/gdwq0506.pdf⟩.
[2] N. Sohel, L.A. Persson, M. Rahman, P.K. Streatfield, M. Yunus, E.C. Ekström, M. Vahter, Epidemiology 20 (2009) 824.
[3] C.Y. Yang, H.F. Chiu, T.N. Wu, H.Y. Chuang, S.C. Ho, Arch. Environ. Health 59 (2004) 484.
[4] C. Hopenhayn-Rich, M.L. Biggs, A.H. Smith, Int. J. Epidemiol. 27 (1998) 561.
[5] C. Ferreccio, C. Gonzalez, V. Milosavjlevic, G. Marshall, A.M. Sancha, A.H. Smith, Epidemiology 11 (2000) 673.
[6] D. Taeger, B. Pesch, J. Occup. Environ. Med. 46 (2004) 1007.
[7] WHO. Guidelines for drinking-water quality, third edition, incorporating first and second addenda. Chemical fact sheets (2006) 306. (⟨http://www.who.int/water_sanitation_health/dwq/GDW12rev1and2.pdf⟩).
[8] International Agency for Research on Cancer (IARC) Monographs on the Evaluation of Carcinogenic Risks to Humans, Supplement 7,1987.
[9] International Programme on Chemical Safety (ICPS) Environmental Health Criteria 224 ARSENIC AND ARSENIC COMPOUNDS. 2001 (⟨http://www.inchem.org/documents/ehc/ehc/ehc224.htm⟩).
[10] A. Manova., E. Beinrohr, F. Cacho, L. Lauko, J. Anal. At. Spectrom. 27 (2012) 695.
[11] N. Tavakkoli, S. Habibollahi, T. Shahla, Chin. J. Chem. 30 (2012) 665.
[12] I. Dol, J. Silva, M. Knochen, M. Pistón, R. Pérez-Zambra, Environ. Geochem. Health 34 (2012) 273.
[13] O Muñiz-Naveiro, A Moreda-Piñeiro, A Bermejo-Barrera, P Bermejo-Barrera, At. Spectroscop. 25 (2004) 79.
[14] M. Colon, M. Hidalgo, M. Iglesias, Talanta 85 (2011) 1941.
[15] M. Rajkumar, S.M. Chen, S. Thiagarajan, Int. J. Electrochem. Sci. 6 (2011) 3164.
[16] A. Mardegan, F. Lamberti, L.M. Moretto, M. Meneghetti, P. Scopece, P. Ugo, Electroanalysis 24 (2012) 798.
[17] L.H. Chen, R.H. Zhu, Asian J. Chem. 23 (2011) 5271.
[18] P.T.K Trang, M Berg, P.H Viet, N Van Mui, J.R van der Meer, Environ. Sci. Technol. 39 (2005) 7625.
[19] E. Majid, S. hrapovic, Y. Liu, K.B. Male, J.H.T. Luong, Anal. Chem. 78 (2006) 762.
[20] J. Orozco, C.F Sanchez, C Jénez-Jorquera, Environ. Sci. Technol. 42 (2008) 4877.
[21] M. Mulvihill, A. Tao, K. Benjauthrit, J. Arnold, P. Yang, Angew. Chem. 120 (2008) 6556.
[22] E.R Forzani, K Foley, P Westerhoff, N Tao, Sens. Actuators 123 (2007) 82.
[23] O Portakal, Turk. J. Biochem. 33 (2008) 35.
[24] R Wilson, Chem. Soc. Rev. 37 (2008) 2028.
[25] N.L Rosi, C.A. Mirkin, Chem. Rev. 105 (2005) 1547.
[26] W Zhao, M.A Brook, Y.F Li, ChemBioChem 9 (2008) 2363.
[27] D.A.Giljohann, D.S.Seferos, W.L.Daniel, M.D. Massich, P.C.Patel, C.A.Mirkin, Angew. Chem. - Int. Ed. 49 (2010) 3280.
[28] T.C Chiu, C.C Huang, Sens.-Basel 9 (2009) 10356.
[29] Y.W Lin, C.W Liu, H.T Chang, Anal. Methods 1 (2009) 14.
[30] M.R Knecht, M Sethi, Anal. Bional. Chem 394 (2009) 33.
[31] Y Lin, C-C Huang, H-T Chang, Analyst 136 (2011) 863.
[32] J. Turkevitch, P.C Stevenson, J Hillier, Discuss. Faraday Soc. 11 (1951) 55.
[33] G Frens, Nature-Phys. Sci. 241 (1973) 20.
[34] M Brust, M Walker, D Bethell, D.J Schiffrin, R Whyman, J. Chem. Soc., Chem. Commun. 0 (1994) 801.
[35] G.K Darbha, A.K Singh, U.S Rai, E Yu, H Yu, P.C Ray, J. Am. Chem. Soc. 130 (2008) 8038.
[36] C.L Schofield, A.H Haines, R.A Field, D.A Russel, Langmuir 22 (2006) 6707.
[37] L Beqa, A.K Singh, S.A Khan, D Senapati, S.R Arumugan, P.C Ray, ACS Appl. Mater. Interfaces 3 (2011) 668.
[38] F. Chai, C Wang, T Wang, L Li, Z Su, ACS Appl. Mater. Interfaces 2 (2010) 1466.
[39] J.R Kalluri, T Arbneshi, S.A Singh, D Senapati, P.C. Ray, Angew. Chem. Int. Ed. 48 (2009) 9668.
[40] X. Ji, X Song, J Li, Y Bai, W Yang, X Peng, J. Am. Chem. Soc. 129 (2007) 13939.
[41] W. Patungwasa, J.H. Hodak, Mater. Chem. Phys. 108 (2008) 45.
[42] Boletín Oficial del Estado, BOE, RD1138/1990.14.